Bachelor Thesis: Dark Matter Signatures in Cosmic γ-rays

Jonas Wessén*
Lund University, Department of Astronomy and Theoretical Physics

Advisors:
José Alberto Ruiz Cembranos, *Universidad Complutense, Madrid, Spain*
Konstancja Satalecka, *Universidad Complutense, Madrid, Spain*
Leif Lönnblad, *Lund University, Sweden*

*E-mail: fys09jwe@student.lu.se

Abstract

This thesis concentrates on one of the indirect Dark Matter (DM) detection methods, namely through observations of Very High Energy (VHE) γ-ray signals from DM annihilation (or decay) in cosmic sources using the Imaging Atmospheric Cherenkov Technique (IACT). We discuss the particle physics and astrophysical aspects of those observations and perform several calculations which lead to an estimation of the DM detection prospects for IACTs. Using the DAMASCO code we calculate the photon flux from annihilating DM. We also calculate the so called astrophysical factors for two promising sources, namely the Galactic Center (GC) and the dwarf galaxy Segue 1. Based on those calculations we examine the prospects for DM detection with the MAGIC telescopes. We conclude that in the best case scenario, a boost factor of ~ 240 is needed for a 5σ detection of the Galactic Center by the MAGIC telescopes during 100 hours of observation. A section is also devoted to the recent tentative measurements of a γ-ray line at ~ 130 GeV, for which we investigate the possibility that it might originate from DM decays. We conclude that such a line can be explained by an unstable particle with a decay time on the order of 10^{28} s, depending on the decay channel, the particle mass and the density distribution of the GC. If the decaying particle is a WIMP (Weakly Interacting Massive Particle), we expect a cut-off in the photon spectra at $E^{\gamma} \approx 260$ GeV. Thereafter, we apply this to a model for decaying gravitinos (supersymmetric partner of the graviton) and calculate value for the relevant coupling. This model predicts a similar line in the neutrino spectrum which could be measured by the IceCube neutrino telescope.

Contents

1 Introduction

There is much experimental evidence indicating that approximately 83% of the total amount of matter is of a form we have not yet encountered, and it is of high priority to unveil the nature of this important building block of the universe. The first chapter in this thesis gives a non-technical overview of the current status of the DM problem, including the experimental evidence for it's existence, the most popular DM candidates and some of the current experiments for direct DM detection.

We thereafter present a more detailed description of indirect DM searches with Imaging Atmospheric Cherenkov Telescopes (IACTs). First, a brief overview over the science of IACTs are given. We then show a derivation of the expected γ-ray flux from annihilating and decaying DM which includes aspects both from particle physics and from astrophysics. This is followed up by a discussion on the dark matter density profiles and a description of the "cusp vs. core" problem. The spectra one expects from DM annihilations depending on the annihilation channel is then discussed. In particular, Chapter 4 describe the implementation of the $t\bar{t}$ annihilation channel in the DAMASCO code, which is used to compute the photon spectra from DM annihilations/decays. Section 2.4 is devoted to the basics of the statistical analysis used in γ-ray astronomy.

We calculate astrophysical factors (for decaying and annihilating DM) for the Milky Way and the dwarf galaxy Segue 1. The astrophysical factors are calculated for typical solid angle resolutions for IACTs and satellite based γ-ray detectors.

The prospects for DM detection with the MAGIC telescopes are then discussed in Chapter 5. Here, we calculate expected γ-ray fluxes from the GC using formulae from Chapter 2. We use the photon spectra computed with the DAMASCO code and use the astrophysical factors for the GC that were calculated in Chapter 3. The flux for different annihilation channels are compared to the γ-ray flux from the Crab nebula and the sensitivity MAGIC achieves in 10 hours or 50 hours of observation time. We thereby calculate the required observation time for 5σ detections assuming different annihilation channels and WIMP masses, and discuss the needed boost factors for the DM γ-ray flux to be detectable with the MAGIC telescopes.

In the last chapter of this work, we analyze the recently observed 130 GeV line in the case it originates from decaying DM. We calculate the life times required for producing this line for the decay channels $\chi \to \gamma\gamma$, $\gamma\nu$, γZ and γh, and the corresponding WIMP masses depending on the density profile applied to the Milky Way. Thereafter, we discuss a model for R-parity violating gravitino decays. By interpreting the 130 GeV line as coming from $\psi_{3/2} \to \gamma\nu$ we obtain the coupling for the corresponding vertex.

2 Overview of the Dark Matter Problem

A variety of experiments show that the forms of matter we know and understand can only constitute a small fraction of all the matter in the universe. From astrophysical measurements such as orbital velocities of stars in galaxies, dynamics of galaxies in galaxy clusters, gravitational lensing effects and anisotropies in the cosmic microwave background (CMB), one can conclude that 83% of the

total mass in the universe (and 23% of the total energy) consists of a form of matter hitherto unknown (see [1], [2] for recent reviews). This "missing mass" is referred to as 'dark matter' (DM) because of historical reasons (the term was coined in order to distinguish the already observed luminous matter from the additional matter that was indirectly inferred by gravitational effects; a more appropriate name would have been 'invisible matter'). The dark matter problem is today considered one of the biggest mysteries in astronomy, cosmology and physics in general.

Even though we do not know what the dark matter is, there exist various observations constraining our theoretical models.

- Since the dark matter is not directly visible in our telescopes (only indirectly through its gravitational effects), it is safe to assume that the dark matter, whatever it is, must have a very tiny coupling to the electromagnetic field, if any at all.

- Dark matter cannot be made up out of any form of baryonic ("ordinary") matter. Physicist can calculate the amount of baryons in the universe by comparing measurements of the ratio between the deuterium and hydrogen abundances with the Big Bang model. Most of the baryons today were created during a period, ranging from a few seconds to a few minutes after the Big Bang, called Big Bang Nucleosynthesis (BBN). Based on measurements of the D/H abundance ratio and the Big Bang model, calculations yield that the baryons only account for about 20% of the total matter density [1]. In accordance with BBN, separate results are independently obtained by calculations based on anisotropies in the CMB. These anisotropies correspond to acoustic oscillations in the photon-proton plasma in the early universe. In the early universe, the temperature was very high preventing electrons and baryons to form atoms. Instead, the universe was a plasma where photons frequently were created and absorbed, maintaining a thermal equilibrium. The acoustic oscillations are the result of a struggle between gravitation, tending the plasma to clump, and radiation pressure from the photons, preventing the clumps from getting to dense. Since the dark matter do not couple to photons, the amount of "clumping" clearly depends on the amount of dark matter present. When the universe expands, the temperature decreases, allowing for neutral atoms to form which makes the universe transparent for photons. Photons then decouple from the rest of the universe and continue to propagate undisturbed by the atoms. These photons now constitute the Cosmic Microwave Background and have been accurately measured most recently by the Wilkinson Microwave Anisotropy Probe (WMAP) satellite [3]. At this "freeze out" of the photons, more photons were present in the denser regions of the photon-proton plasma. The anisotropies in the CMB therefore directly shows the density fluctuations in the early universe photon-proton plasma which, in turn, crucially depends on the amount of dark matter density and baryonic matter density. The measurements of the CMB predict that the matter in the universe today is made up of 83% of dark matter [3], in accordance with the prediction from BBN.

- The results of rigorous cosmological simulations, in which it is assumed that DM is a new elementary particle, favor the so called Cold Dark Matter

model (ΛCDM) when compared to the universe we observe. The observed large-scale structure only appears when the dark matter is cold, meaning that its kinetic energy is negligible compared to its energy at rest. In most cases, this implies that the dark matter particle must be very heavy. One exception is the so called *axion* which is a light ($m \leq 1$ eV) boson which is proposed in Quantum Chromo Dynamics (QCD), the theory of the strong force, in order to solve the strong CP problem; it would be produced without kinetic energy meaning that the axion still satisfies this criteria despite its low mass.

- Another important piece of information about the dark matter can be obtained from cosmology regarding its (thermally averaged) annihilation cross-section $\langle \sigma v \rangle$, assuming a thermally produced DM particle (again, the axion is an example of a DM candidate for which the following argument does not hold, since it is not thermally produced). When the universe was young it was both hot and dense causing frequent interactions between particles. DM particles should have been frequently created and annihilated pairwise, maintaining the right number density and temperature for thermal equilibrium. When the universe expands, both the temperature and the number density drops, having the effect that the annihilation reaction rate also drops. The dark matter density today depends on the amount of dark matter present at the time when the rate of annihilation had fallen to a value for which thermal equilibrium could no longer be maintained. Since the annihilation rate equals the annihilation cross-section times the number density, one can estimate the cross-section assuming a dark matter particle mass. It turns out that the amount of dark matter we believe exist today is consistent with a heavy particle (a mass in the GeV to TeV range) with $\langle \sigma v \rangle \sim 3 \cdot 10^{-26} \text{cm}^3/\text{s}$ (see [4] for a recent calculation) which is close to the electro-weak scale. Because of this reason, a popular class of dark matter candidates are the so called *Weakly Interacting Massive Particles*, WIMPs, referring to heavy non-baryonic particles which only interacts through weak interactions. An interesting note here is that the Fermi telescope claims to have ruled out this cross-section for $b\bar{b}$ and $\tau\bar{\tau}$ annihilation channels for a WIMP mass ranging from 5 GeV to about 30 GeV by using standard assumptions [5] (their results are shown in Fig. 1).

In the particle physics community, a common belief is that the so called *Standard Model* (SM) of particle physics is only a part of a more general theory, which should be unveiled at high energies. Although the Standard Model as a theory has offered an astonishing agreement with experiments, it possesses quite a lot of theoretical problems (for example the hierarchy problem, neutrino masses or the uncomfortably large number of free parameters), and attempts have been made to solve these problems by extending the Standard Model.

A favorited category of possible extensions to the standard model are the *Super Symmetric* models, or SUSY models. The 'symmetry' in SUSY refers to a proposed symmetry between fermions and bosons – for every SM fermion there exists a boson with identical mass and quantum numbers (except the spin) referred to as the 'sfermion', and vice versa for the SM bosons for which the supersymmetric partners are called 'gauginos' (see Tables 1 and 2). Since we have never seen any of these sfermions and gauginos, this symmetry cannot be an

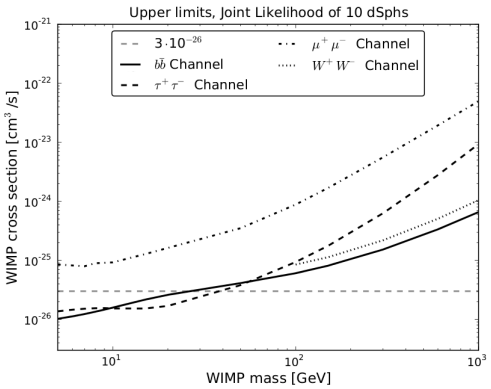

Figure 1: Upper limits on the WIMP annihilation cross-section from the Fermi Large Area Telescope [5].

exact symmetry if it exists. If Nature is supersymmetric, the explanation yields that SUSY is broken in such a way that all the superpartners of the standard model particles have such high masses that no particle physics experiment so far has had enough energy available to create a superpartner to any SM particle.

In SUSY, it is possible to introduce the quantum number R-parity P_R for which all SM particles have $P_R = 1$, and $P_R = -1$ for their supersymmetric partners. A definition of R-parity which acquires this property is

$$P_R = (-1)^{2s+3(B-L)}$$

where s is the spin, B the baryon number and L the lepton number. Thus, by this definition, a violation of R-parity implies a violation of $B - L$ which in many cases opens up the possibility of a proton decay (see for example [7] for a discussion on the consequences of R-parity violation). The proton decay has not yet been observed; the experimental lower limit for the proton half life is of order 10^{33} s [8], i.e. much longer than the age of the universe which is around 10^{17} s. However, in the Minimal SuperSymmetric Model, MSSM, there is no fundamental reason why R-parity should exactly be conserved. Even though the lightest supersymmetric particle, the LSP, would not be stable in the R-parity violating case, the lifetime of the LSP can be extremely long provided that the R-parity violation is small enough. For example, if the gravitino is the LSP it has been shown that the problem of gravitino overproduction in the early universe can be solved by introducing a small R-parity violation and still leave the gravitino constituting the DM bulk today (see [9] for a more detailed discussion on gravitino dark matter).

The usual LSP in SUSY models is the lightest neutralino, since it naturally provides a good dark matter candidate (it also common to consider the case where the gravitino is the LSP). The neutralino is a superposition of the superpartners of the gauge bosons and higgses in the Standard Model which lacks both electric and color charge. It is thus only interacting via the weak force, and usually has a mass in the right range. In addition, the neutralino is a Majorana

Particle	Mass(GeV)
up squark ($\tilde{u}$)	> 379
down squark ($\tilde{d}$)	> 379
selectron ($\tilde{e}$)	> 107
e neutrino ($\tilde{\nu}_e$)	> 94
charm squark ($\tilde{c}$)	> 379
strange squark ($\tilde{s}$)	> 379
smuon $\tilde{\mu}$	> 94
μ sneutrino ($\tilde{\nu}_\mu$)	> 94
top squark ($\tilde{t}$)	> 95.7
bottom squark ($\tilde{b}$)	> 89
stau ($\tilde{\tau}$)	> 81.9
τ sneutrino ($\tilde{\nu}_\tau$)	> 94

Table 1: Sfermions and their lower mass limits last reported by the Particle Data Group [6].

Particle	Mass(GeV)	Description
Neutralinos ($\tilde{\chi}^0_{1-4}$)	> 46	Linear combinations of the photino ($\tilde{\gamma}$), the zino ($\tilde{Z}$) and the two neutral higgsinos ($\tilde{H}^0_{1,2}$)
Charginos ($\tilde{\chi}^\pm_{1,2}$)	> 94	Linear combinations of winos($\tilde{W}^\pm$) and charged higgsinos ($\tilde{H}^\pm$)
Gluinos ($\tilde{g}$)	> 308	Superpartners to the gluons
Gravitino ($\psi_{3/2}$)	-	Superpartner to the postulated mediator of the gravitational force, the graviton. The subscript 3/2 emphasizes the spin of the gravitino.

Table 2: Gauginos and their lower mass limits last reported by the Particle Data Group [6].

fermion, meaning that it is its own antiparticle. This is crucial when considering γ-rays originating from annihilating dark matter since an annihilation reaction is a reaction between a particle and its antiparticle. If the dark matter bulk of the universe is not made out of particles with this property, and if the dark matter possesses the same matter-antimatter asymmetry as the matter we know of today, there is little hope of ever detecting γ-rays from DM annihilations.

Another set of models that are often discussed in the context of DM are the *Kaluza-Klein* models which, in addition to our 3 spatial dimensions, postulates extra spatial dimensions which are "curled up" and usually extremely small. Imposing the requirement of a continuous wave function of a particle moving in one of these dimensions leads to a discrete set of energy eigenstates, or "Kaluza-Klein modes". Conservation of momentum in the extra dimensions leads to a conserved quantum number called KK-parity, which in turn leads to stable modes which are considered as DM candidates.

Much work has been done in DM detection, and many interesting experimental results are expected in the upcoming years. The different techniques for detecting dark matter are usually divided up into two categories: *direct* and *indirect* detection. This work focuses on indirect detection of DM via detection of high energy γ-rays presumably produced by DM annihilation or decay, but for the sake of completeness, other techniques will hereby briefly be mentioned.

In the Large Hadron Collider (LHC) at CERN, searches for supersymmetry are currently conducted. No signatures have been seen yet, but lower limits for the sparticles have been set (see Tables 1 and 2).

Another method for direct detection of is employed by experiments such as CDMS, ZEPLIN and DAMA. The idea is to detect recoil events from elastic scattering of WIMPs against nucleons in the detectors. Since these events would occur very seldom due to the low cross-section and the low number density of the WIMP, the detectors must be extremely cold (around 10 mK) in order for the thermal motion not to overshadow the recoil event, and be placed deep underground to avoid background in the form of cosmic radiation. So far, no convincing claims of detecting such events have been made. A compilation of upper limits for the WIMP-nucleon cross-section is shown in Fig. 2.

The rest of this thesis will mainly focus on indirect DM detection with γ-rays using Imaging Atmospheric Cherenkov Telescopes. Other experiments attempting to detect DM annihilation products are the IceCube neutrino detector located on the South Pole, the Fermi Large Area Telescope (LAT) and the PAMELA satelite, both located in space.

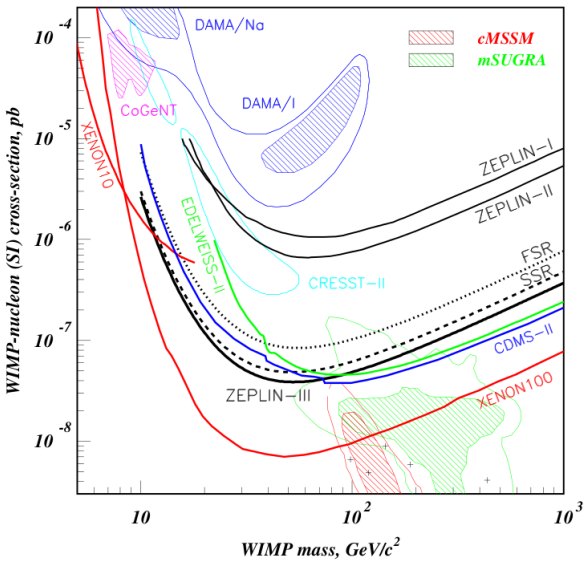

Figure 2: Upper limits on the WIMP-nucleon cross-section from various experiments dealing with direct detection of WIMPs through registration of recoil events from WIMP-nucleon elastic scattering. Preferred cross-sections in the SUSY models cMSSM and mSUGRA are shown in the red and green regions respectively. The regions DAMA/No, DAMA/I and CoGeNT show three claims of DM detection which have not been confirmed. The figure was extracted from [10].

3 Indirect Dark Matter Searches in γ-ray Astronomy

Assuming that the dark matter constituent is a WIMP with an expected mass of a few 100 GeV to several TeV, one expects to observe a flux of high energy (HE) photons, with an energy in the GeV-TeV range, coming from DM rich regions in space. Those γ's, along with other particles, are products of DM annihilation or decay processes. In contrast to the charged particles, photons have the advantage that they do not bend in magnetic fields, making it easy to trace them back to their origin.

3.1 The Imaging Atmospheric Cherenkov Technique

HE photons are only possible to directly detect with space satellites or balloons, since the photons will be absorbed once they reach the Earth's atmosphere. However, once a HE γ reaches the atmosphere, it will interact with air molecules producing an e^+e^--pair followed by an electromagnetic shower. Some of the particles in such a cascade will have a velocity higher than the speed of light in air (which is c/n where n is the refractive index in air). If the particle is also charged, it will radiate Cherenkov light. The minimum energy required for a charged particle to emit Cherenkov light is thus

$$E_{\text{Min}} = \frac{m_0 c^2}{\sqrt{1 - \frac{1}{n^2}}}.$$

The purpose of Imaging Atmospheric Cherenkov Telescopes, or IACTs, is to detect Cherenkov radiation from air showers induced by γ-rays interacting with air molecules in the Earth's atmosphere (see Figure 3). The Cherenkov photons are reflected in the mirrors, and the shower image is recorded by a camera made by photomultipliers. Hadronic showers induced by charged cosmic rays (mainly protons) produce similar images and constitute the main background for γ-ray detection. The shape of the shower, the arrival time of the Cherenkov photons and the amplitude of the signal is analyzed in order to extract information about the primary and to discriminate the photons from the background. Figure 4 shows three typical kinds of events recorded by an IACT, before and after the the image cleaning[1].

It is of great benefit to have several IACTs simultaneously active. The cooperation of multiple IACTs simplifies the reconstruction of the shower arrival direction thanks to their stereoscopic perspective. The full Cherenkov light pool illuminates a large area of the ground compared to the individual areas of the telescopes (the Cherenkov light originating from a primary γ-ray with an energy of $\sim$1 TeV illuminates a circle of a radius $\sim$100 m when it reaches the ground). By having several telescopes in the light pool, one of course collects more information about the primary γ which gives a more accurate estimation of its energy.

IACTs are mainly used to study galactic objects such as supernova remnants (SNR) and pulsars, and extra-galactic objects such as active galactic nuclei

[1]Image cleaning is a procedure which removes obsolete signals coming from the night sky background (starlight, moonlight, light pollution etc.), electronic noise and other random events.

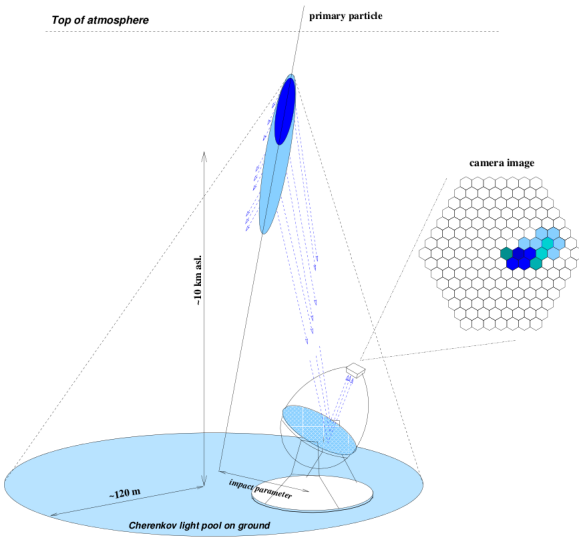

Figure 3: A primary HE photon enters the Earths atmosphere and produces particle shower. The charged particles in the shower with sufficiently high energy will emit Cherenkov radiation which is detected by an IACT. The picture is from [11].

(AGN) and Gamma Ray Bursts (GRBs). In the last years, more and more of the IACTs observation time is dedicated to study exitic phenomena such as DM and Lorentz invariance violation predicted by some theories of Quantum Gravity (see for example [12]).

This work will mainly focus on DM detection prospects for the Major Atmospheric Gamma Imaging Cherenkov (MAGIC) telescopes. The MAGIC telescopes are two 17 m diameter IACTs located on the Canary island La Palma (Spain) providing a stereoscopic view on the VHE γ-ray sky of the northern hemisphere. Among the active IACTs today, MAGIC has the lowest energy threshold and best sensitivity below 150 GeV, which is especially important in WIMP detection where the WIMP has a relatively low mass (100-200 GeV).

In DM searches with IACTs, several types of objects are considered promising candidates: the Galactic Center (GC), the galaxy clusters, the Dwarf Shperoidal Galaxies (dShps) and the UFOs (Unassociated Fermi Objects).

The Galactic Center (GC) is comparably near the Earth ($\sim$8.5 kpc) and is expected to have a high dark matter concentration. However, since the GC in addition contains a lot of forms of luminous matter, there is a difficulty in ruling out less exotic VHE gamma-ray sources of astrophysical origin. So far, no detection with IACTs has been claimed (see for example [15]).

The dSphs are gravitationally bound systems that are present inside the dark matter halo of the Milky Way. They have a low luminosity since they contain very few stars, but high masses which point to high DM concentrations [13]. In addition to their high mass-to-light ratio, dSphs are usually located outside the galactic plane which makes the background estimation less complicated. No claim of VHE γ-ray detection with an IACT has been made (see for example

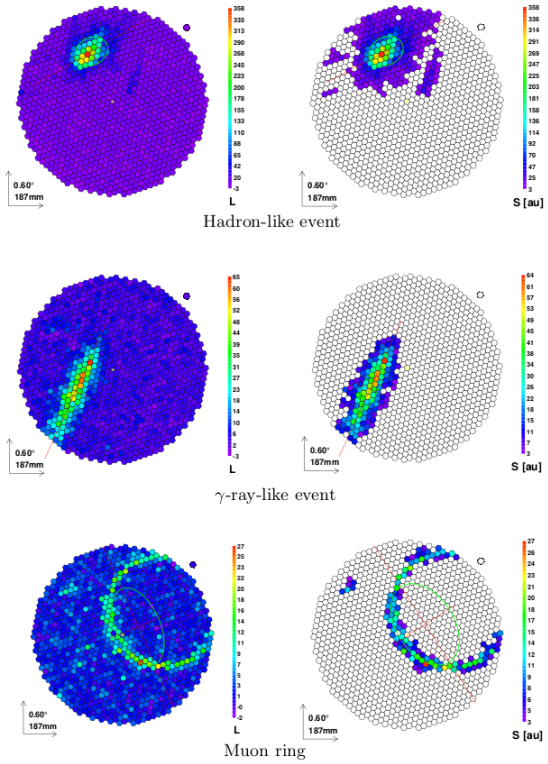

Figure 4: The picture shows three types of events recorded by an IACT, before and after the image cleaning. The picture is from [11].

[16]).

Galaxy clustes have been shown to have a high mass-to-light ratio which is good for indirect DM searches. Their disadvantage is their large distance from the Earth. MAGIC has attempted to detect γ-rays from galaxy clusters with IACTs, but no signal was seen (see for example [14]).

Cosmological Cold Dark Matter N-body simulations suggest that galaxies like our own are surrounded by many subhalos of all mass scales [17]. Part of these subhalos could be too small to have attracted enough baryonic matter to start star formation and would therefore be invisible to traditional observations. Those sources are expected to shine exclusively in the γ-ray regime where a DM annihilation/decay signal is expected. Not detected in any other wavelength, they could pop-up in all-sky monitoring programs, such as the one carried out by Fermi-LAT. The Dark Matter subhalos might therefore correspond to some of the so called Unassociated Fermi Objects (UFOs) which have no precise association to any counterpart in other wavelengths. Attempts have been made to measure a γ-ray signal from UFOs with the MAGIC telescopes, but no detection was claimed [18].

3.2 γ-ray Flux from Annihilating and Decaying Dark Matter

In order to estimate the photon flux coming from dark matter annihilation or decay, one needs to take into account both astrophysical models for the DM density distribution and particle physics models for the relevant cross-sections and decay widths.

Assume that a telescope with an angular opening of $2\theta_{max}$, corresponding to a solid angle resolution of $\Delta\Omega = 2\pi(1-\cos\theta_{max})$, is observing an object (for example a dSph) whose center is at a distance D from the telescope. This means that photons can be detected, only if they were emitted in the right direction inside a cone with opening angle $2\theta_{max}$ directed along the line of sight of the telescope.

The rate at which WIMPs annihilate in a volume $\mathrm{d}V = l^2\mathrm{d}l\mathrm{d}\Omega$, where l is the distance from the telescope, may be estimated as follows. Let M be the WIMP mass and $\rho[r(l)]$ be the dark matter density at a distance r from the center of the dark matter halo, meaning that $r = \sqrt{D^2 + l^2 - 2Dl\cos\theta}$, where θ is the azimuth angle. The thermally averaged cross-section for annihilation channel i is denoted by $\langle\sigma_i v\rangle$, meaning that the annihilation rate per particle is

$$\sum_i^{\text{channels}} \frac{\rho[r(l)]}{M} \cdot \langle\sigma v_i\rangle,$$

where the sum is taken over all annihilation channels. The total annihilation rate in $\mathrm{d}V$ is then given by the the annihilation rate per particle times the number of pairs of particles in $\mathrm{d}V$ (since two particles participate in every reaction), i.e.

$$\left(\sum_i^{\text{channels}} \frac{\rho[r(l)]}{M} \cdot \langle\sigma_i v\rangle\right) \cdot \left(\frac{\rho[r(l)]\mathrm{d}V}{2M}\right).$$

Let the differential energy spectrum of γ's from a single reaction in annihilation channel i be denoted by $\mathrm{d}N_i^\gamma/\mathrm{d}E$. The differential flux coming from $\mathrm{d}V =$

$l^2 \mathrm{d}l\mathrm{d}\Omega$ at a distance l is then

$$\frac{1}{4\pi l^2} \sum_i^{\text{channels}} \frac{\mathrm{d}N_i^\gamma}{\mathrm{d}E} \cdot \frac{\langle \sigma_i v \rangle \rho^2[r(l)]}{2M^2} l^2 \mathrm{d}l\mathrm{d}\Omega.$$

Integrating over the whole volume in the cone in which we observe, one obtains the differential photon-flux from annihilating dark matter that is expected to be measurable:

$$\begin{aligned} \frac{\mathrm{d}\Phi_{\mathrm{A}}^\gamma}{\mathrm{d}E} &= \int_{\Delta\Omega} \mathrm{d}\Omega \int_{\text{l.o.s.}} \mathrm{d}l \sum_i^{\text{channels}} \frac{\mathrm{d}N_i^\gamma}{\mathrm{d}E} \cdot \frac{\langle \sigma_i v \rangle \rho^2[r(l)]}{8\pi M^2} \\ &= \underbrace{\frac{1}{8\pi M^2} \sum_i^{\text{channels}} \frac{\mathrm{d}N_i^\gamma}{\mathrm{d}E} \langle \sigma_i v \rangle}_{\text{Particle physics dependent}} \times \underbrace{\int_{\Delta\Omega} \mathrm{d}\Omega \int_{\text{l.o.s.}} \mathrm{d}l \rho^2[r(l)]}_{\text{Astrophysics dependent}} \end{aligned} \tag{1}$$

where the second integral is performed along the line of sight (l.o.s) to the target. The astrophysics part of Eq.(1) is commonly referred to as the "astrophysical factor" $J_{\mathrm{A}}(\Delta\Omega)$, which is often expressed as $J_{\mathrm{A}}(\Delta\Omega) = \Delta\Omega \langle J_{\mathrm{A}} \rangle_{\Delta\Omega}$, where of course

$$\langle J_{\mathrm{A}} \rangle_{\Delta\Omega} = \frac{1}{\Delta\Omega} \int_{\Delta\Omega} \mathrm{d}\Omega \int_{\text{l.o.s.}} \mathrm{d}l \rho^2[r(l)]. \tag{2}$$

In a similar fashion, it is straight forward to derive the flux from decaying dark matter:

$$\frac{\mathrm{d}\Phi_{\mathrm{D}}^\gamma}{\mathrm{d}E} = \underbrace{\frac{1}{4\pi M} \sum_i^{\text{channels}} \Gamma_i \frac{\mathrm{d}N_i^\gamma}{\mathrm{d}E}}_{\text{Particle physics dependent}} \times \underbrace{\int_{\Delta\Omega} \mathrm{d}\Omega \int_{\text{l.o.s.}} \mathrm{d}l \rho[r(l)]}_{\text{Astrophysics dependent}} \tag{3}$$

where Γ_i is the decay width of decay channel i. The astrophysics part of Eq. (3) is referred to as the astrophysical factor for decaying dark matter, labeled $J_{\mathrm{D}}(\Delta\Omega) = \Delta\Omega \langle J_{\mathrm{D}} \rangle_{\Delta\Omega}$, where

$$\langle J_{\mathrm{D}} \rangle_{\Delta\Omega} = \frac{1}{\Delta\Omega} \int_{\Delta\Omega} \mathrm{d}\Omega \int_{\text{l.o.s.}} \mathrm{d}l \rho[r(l)] \tag{4}$$

is $J_{\mathrm{D}}(\Delta\Omega)$ averaged over the solid angle $\Delta\Omega$.

3.3 Dark Matter Density Profiles

After many years of successive Monte Carlo simulations and experimental measurements, the scientific community has still not reached a consensus of what the most accurate profile is. Assuming a spherical distribution, the most commonly used profile is the *Navarro-Frenk-White* profile (hereafter referred to as "NFW") [19]

$$\rho(r) = \frac{\rho_{NFW}}{(r/r_{NFW})(1 + r/r_{NFW})^2} \tag{5}$$

where r is the distance from the center of the DM distribution, and the parameters ρ_{NFW} and r_{NFW} define a characteristic density and distance scale.

Two other frequently used profiles are the *Moore* profile

$$\rho(r) = \frac{\rho_M}{(r/r_M)^{1.5}[1 + (r/r_M)^{1.5}]} \tag{6}$$

with parameters ρ_M and r_M, and the *Einasto* profile

$$\rho(r) = \rho_E \exp\left\{-\frac{2}{\alpha}\left[\left(\frac{r}{r_E}\right)^{\alpha} - 1\right]\right\} \tag{7}$$

with parameters ρ_E, r_E and α which is usually in the range $0.1 - 0.3$ [20]. Both the Moore profile and the Einasto profile are described in [20]. According to [20], the parameters in these three profiles are related by

$$r_{NFW} = r_E = 2^{-2/3} r_M, \tag{8}$$

$$\rho_{NFW} = 4\rho_E = \frac{16}{3}\rho_M. \tag{9}$$

These three profiles are all obtained by parameterizing density distributions obtained by Monte Carlo simulations within the framework of the ΛCDM model. The NFW, the Einasto and the Moore profiles are classified as "cusped" profiles due to their steep slope around $r = 0$.

A possible discrepancy between the ΛCDM model and observations should here be pointed out. Even though ΛCDM can explain large-scale structure formation, it is questionable if it describes the structure on smaller scales, such as the dark matter halo density profiles. Simulations based on the ΛCDM model seem to indicate a cusped profile [20], but some authors (see for example [21]) claim that a constant central density better fits the observed rotation curve of the Milky Way. A density profile with a constant central density is called a *cored* profile. Examples of popular cored profiles are the isothermal density profile

$$\rho(r) = \frac{\rho_I}{1 + (r/r_I)^2} \tag{10}$$

and the Burkert profile

$$\rho(r) = \frac{\rho_B}{[1 + r/r_B)(1 + (r/r_B)^2]}, \tag{11}$$

which both has a constant density around $r = 0$. Figure 5 shows the NFW, Moore, Einasto and Isothermal density profiles, with parameters corresponding to the Milky Way DM halo.

Whether or not the density profiles are cored or cusped makes a large impact on the γ-flux we hope to detect, especially in the case of annihilating dark matter. Assuming the telescope is pointing directly towards the center of the DM distribution (which is the usual assumption when calculating the astrophysical factors), the point $r = 0$ will be included in the integrals in Eqs.(2) and (4). In the case of a cusped profile, the region around $r = 0$ will be very dense, resulting in a high flux of photons, much higher than if the profile were to be cored. The difference is extra prominent in the case of annihilating dark matter since the integrand in Eq.(2) is the density squared.

The cuspiness of halos seen in ΛCDM simulations can actually be reduced (but not removed) taking decaying dark matter into account. In [22], a simple

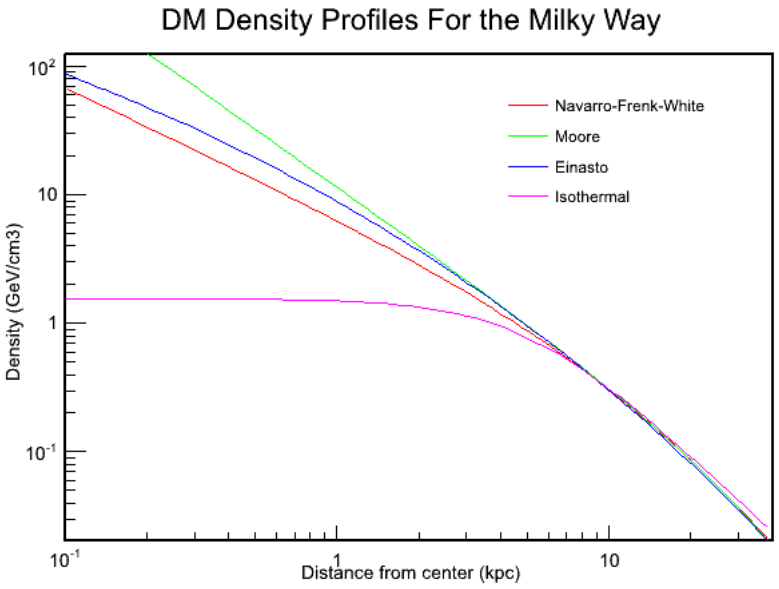

Figure 5: Several density profiles for the DM halo in the Milky Way. The parameters for the profiles taken from in [28].

cosmological model with decaying cold dark matter is presented, ΛDCDM, in which it is shown that the central density of dark matter halos is decreased compared to halos in ΛCDM. The cold dark matter particles decay to relativistic particles (which therefore are able to leave the gravitational field of the halo), causing a change in the gravitational potential which in turn results in an adiabatic expansion of the halo. In addition, the inclusion of decaying dark matter in ΛCDM offers a solution to the problem of the over-concentration of dark matter and the over-abundance of dwarf galaxies present in ΛCDM simulation [22]. This provides a strong motivation for studying decaying dark matter, even though one should keep in mind that decaying dark matter is an exotic idea in the context of SUSY most models. For a more detailed discussion on the "core/cusp" problem, see [13] and [23].

3.4 Photon Spectra from DM Annihilation and DM Decay

In the usual case where the dark matter particle do not couple to photons, annihilation channels such as $\chi\chi \to \gamma\gamma$ are loop suppressed and will therefore have a small branching ratio. The normal situation in WIMP models is that two WIMPs annihilate into to a particle-antiparticle pair of SM particles (which aren't photons), and which in turn produce photons after decays and/or hadronization of unstable products such as quarks and leptons. The emitted photons will therefore constitute a continuous spectra, $\mathrm{d}N^{\gamma}/\mathrm{d}E$, but with a cut-off at m_{χ}. Take for example the reaction $\chi\chi \to b\bar{b}$. In the rest frame, the total energy will be approximately $2m_{\chi}$ since the dark matter particles should be non-relativistic (due to their high mass and low temperature), so that each

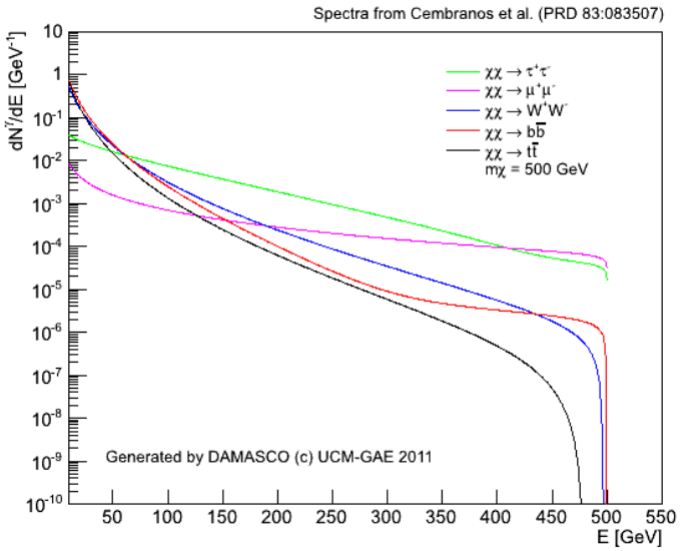

Figure 6: Photon spectra from WIMP annihilations generated by the DAMASCO web application for a 500 GeV WIMP mass.

quark gets a total energy of m_χ. Treating m_χ as a parameter, the photon spectra of a $b\bar{b}$-pair each with energy m_χ can then be obtained from Monte Carlo simulations in the well known Pythia package [30]. In [31], such simulations has been conducted for the $W^+W^-, Z^0Z^0, t\bar{t}, \tau^+\tau^-, \mu^+\mu^-, u\bar{u}, d\bar{d}, s\bar{s}, c\bar{c}, b\bar{b}$ channels along with analytical fits for $\mathrm{d}N^\gamma/\mathrm{d}E$ for each channel. Based on this work, a code for calculating the DM spectra is publicly available as the web application DAMASCO[2] (DArk Matter Analytical Spectral COde). In DAMASCO, the photon spectra from the annihilation channels $W^+W^-, \tau\bar{\tau}, \mu\bar{\mu}, b\bar{b}$ are implemented, as well as the $t\bar{t}$ channel which we implemented as a part of this work (this is described in more detail in chapter 4). An example of a spectrum generated by DAMASCO is shown in Fig.6.

Note that the flux in Eq.(1) depends on the sum

$$\sum_i \langle \sigma_i v \rangle \frac{\mathrm{d}N_i^\gamma}{\mathrm{d}E}$$

where the $\langle \sigma_i v \rangle$'s are to be obtained from a particle physics model. The measured flux will not directly give the $\langle \sigma_i v \rangle$'s, and it can therefore be very hard to accurately disentangle the $\langle \sigma_i v \rangle$'s from the experimental data in order to confirm or reject particular details in the WIMP model used. However, all spectra in Fig.6 show a cut-off at an energy $E_\gamma \sim m_\chi$, since photons with an energy larger than m_χ cannot be produced due to conservation of energy. Such a cut-off could be a clear experimental signature of dark matter, although less exotic

[2]The DAMASCO software is available as a web-application on http://cta.gae.ucm.es/gae/damasco.

explanations first should be ruled out (a cut-off in the photon spectra could also be explained by an absorption process).

In the case of a loop suppressed annihilation into a photon and an additional particle X, i.e. $\chi\chi \to \gamma X$, the energy of the photon, E_{A}^{γ} can be calculated by simple relativistic kinematics. Let the two DM particles in the rest frame have four-momentum $p^{\mu} = (E_{\chi}, \vec{p})$ and $p'^{\mu} = (E_{\chi}, -\vec{p})$. The photon has four-momentum $q_{\gamma}^{\mu} = (E_{\mathrm{A}}^{\gamma}, \vec{q})$ and the particle X has $q_{X}^{\mu} = (E_{X}, -\vec{q})$. Conservation of four-momentum leads to

$$p^{\mu} + p'^{\mu} - q_{\gamma}^{\mu} = q_{X}^{\mu}.$$

Squaring both sides gives

$$2m_{\chi}^2 + 2E_{\chi}^2 - E_{\chi}E_{\mathrm{A}}^{\gamma} = m_{X}^2.$$

Assuming a cold dark matter particle, i.e. $E_{\chi} \sim m_{\chi}$, the above expression simplifies to

$$E_{\mathrm{A}}^{\gamma} = m_{\chi}\left(1 - \frac{m_{X}^2}{4m_{\chi}^2}\right). \tag{12}$$

Similarly, for decaying dark matter where χ decays to a photon and another particle X, the photon energy is given by

$$E_{\mathrm{D}}^{\gamma} = \frac{m_{\chi}}{2}\left(1 - \frac{m_{X}^2}{m_{\chi}^2}\right). \tag{13}$$

Although $\chi\chi \to \gamma X$ is typically loop suppressed, it may still give a detectable signal since the shape of the spectra is that of a delta function, i.e.

$$\frac{\mathrm{d}N_{\chi\chi\to\gamma X}^{\gamma}}{\mathrm{d}E} = a\delta(E - E_{\mathrm{A}}^{\gamma}) \tag{14}$$

where E_{A}^{γ} is given by Eq.(12), and $a = 2$ for the case where X is a photon and $a = 1$ otherwise. These processes, which produce monochromatic photons, should thus give a sharp peak in the measured differential flux. Even though the underlying process is typically loop suppressed, it may actually be easier to observe since its signature (a peak) is much easier to identify in contrast to the type of diffuse photon spectra that are shown in Figure 6.

The spectra resulting from decaying dark matter is calculated in DAMASCO, replacing m_{χ} by $m_{\chi}/2$ since the CM energy is half of the energy in the corresponding annihilation. Hence, the spectra of a DM decay can also exhibit the characteristic cut-off, but now at $E_{\gamma} = m_{\chi}/2$.

The usual case considered is that the photons from $\chi\chi \to \gamma\gamma$ are coming from a loop of a charged SM fermion meaning that, if one chooses such an interpretation of a line in a measured spectra, one should also expect a reaction such as $\chi\chi \to \gamma Z$ to happen in most cases. According to Eq.(12), it should therefore be possible to dissolve a measured line into two lines, separated by an energy of $m_{Z}^2/(4m_{\chi})$. For a deeper discussion on the number of lines expected from DM annihilations, see [32]. However, it is typically hard to identify the two lines due to the resolution of the telescopes.

Similarly to Eq.(14), the differential spectra for the decay $\chi \to \gamma X$ is

$$\frac{\mathrm{d}N_{\chi\to\gamma X}^{\gamma}}{\mathrm{d}E} = a\delta(E - E_{\mathrm{D}}^{\gamma}) \tag{15}$$

where E_{D}^{γ} is given by Eq.(13).

3.5 Statistical Analysis in γ-ray Astronomy

In this section, we discuss a formula for calculating the significance of γ-ray observations when taking into account the background.

A typical measurement of VHE γ-rays consist of exposing an IACT to the suspected source for a time $t_{\rm obs}$, and then pointing the telescope towards an "empty" patch of the sky during a time $t_{\rm obs}/\alpha$ to measure the background radiation (α is the ratio between the time spent on the source, and the time spent on measuring the background). In this work we only treat the simple case where $\alpha = 1$, but a comment on the general case $\alpha \neq 1$ will be made.

Let $N_{\rm on}$ be the number of photons observed when the telescope is directed towards the source, and $N_{\rm off}$ the number of photons registered when measuring the background. For $\alpha = 1$, we have

$$N_{\rm on} = N_{\rm exc} + N_{\rm off}, \tag{16}$$

where $N_{\rm exc}$ is the number of photons that is attributed to the source. Often, $N_{\rm exc} \ll N_{\rm off}$, meaning that the total number of photons detected to a good approximation equals $2N_{\rm off}$. The significance S is the ratio between the number of excess photons and the standard deviation of the total photon distribution which is estimated as $\sqrt{2N_{\rm off}}$.

$$S = \frac{N_{\rm exc}}{\sqrt{2N_{\rm off}}}. \tag{17}$$

This approach works in the special case $\alpha = 1$, and is an approximation of a more general formula derived in [29],

$$S = \sqrt{2}\left\{N_{\rm on}\ln\left[\frac{1+\alpha}{\alpha}\left(\frac{N_{\rm on}}{N_{\rm on}+N_{\rm off}}\right)\right] + N_{\rm off}\ln\left[(1+\alpha)\left(\frac{N_{\rm off}}{N_{\rm on}+N_{\rm off}}\right)\right]\right\}^{1/2},$$

which is used as a standard for evaluating the significance of a measurement in γ-ray astronomy. The expression above indeed approaches Eq.(17) in the limit $N_{\rm exc} \ll N_{\rm off}$.

To obtain the observation time $t_{\rm obs}$ required for a significance S, we first express $N_{\rm exc}$ and $N_{\rm off}$ as

$$N_{\rm exc} = t_{\rm obs}R_{\rm exc}, \tag{18}$$

$$N_{\rm off} = t_{\rm obs}R_{\rm off}, \tag{19}$$

where $R_{\rm exc}$ and $R_{\rm off}$ are the rates at which excess photons and background photons are detected. Solving Eq. (17) for $t_{\rm obs}$ gives

$$t_{\rm obs} = 2S^2\frac{R_{\rm off}}{R_{\rm exc}^2}. \tag{20}$$

4 Implementation of the $t\bar{t}$ Annihilation Channel in DAMASCO

As previously mentioned, DAMASCO (DArk Matter Analytical Spectral COde) is a ROOT based tool for calculating the photon spectrum $\mathrm{d}N^\gamma/\mathrm{d}E$ emerging from a SM particle-antiparticle pair that is produced with a total energy of m_χ in the rest frame. These spectra are needed in order to predict the photon flux coming from annihilating or decaying dark matter, Eq.(1) and Eq.(3).

An introductory task for this work was to implement a new annihilation channel in the DAMASCO application, namely the $\chi\chi \to t\bar{t}$ channel. Following [31], the differential photon spectra $\mathrm{d}N^\gamma/\mathrm{d}E$ from the processes following of the $t\bar{t}$ production, with a total center of mass energy of m_χ, is parameterized by

$$x^{1.5}\frac{\mathrm{d}N^\gamma}{\mathrm{d}x} = a_1 \exp\left[-b_1 x^{n_1} - \frac{c_1}{x^{d_1}} - \frac{c_2}{x^{d_2}}\right]\left\{\frac{\ln[p(1-x^l)]}{\ln p}\right\}^q \tag{21}$$

where

$$x = \frac{E}{m_\chi}. \tag{22}$$

The parameters

$$a_1 = 290, \tag{23}$$
$$c_1 = 1.61, \tag{24}$$
$$d_1 = 0.19, \tag{25}$$
$$d_2 = 0.845, \tag{26}$$

turn out to be independent of the WIMP mass m_χ, whereas the other parameters are fitted by power laws in m_χ,

$$b_1 = \begin{cases} 9.32 m_\chi^{0.0507} + 11.0 \cdot 10^6 m_\chi^{-2.91}, & 200\mathrm{GeV} \le m_\chi \le 350\mathrm{GeV} \\ 16.4 m_\chi^{-0.400}, & 350\mathrm{GeV} < m_\chi \le 1000\mathrm{GeV} \end{cases} \tag{27}$$

$$n_1 = \begin{cases} 21.4 m_\chi^{-0.818} + 0.000867 m_\chi^{0.589}, & 200\mathrm{GeV} \le m_\chi \le 300\mathrm{GeV} \\ 0.559 m_\chi^{-0.0379}, & 300\mathrm{GeV} < m_\chi \le 1000\mathrm{GeV} \end{cases} \tag{28}$$

$$c_2 = 8910 m_\chi^{-3.23}, \tag{29}$$
$$p = 5.78 \cdot 10^{-5} m_\chi^{1.89}, \tag{30}$$
$$q = 0.133 m_\chi^{0.488}, \tag{31}$$
$$l = 21.9 m_\chi^{-0.302}, \tag{32}$$

where Eqs.(30)-(32) are valid for a WIMP mass in the range between 200 GeV and 1000 GeV. See Figure 7 for the analytical fit compared to the Pythia simulation of $\chi\chi \to t\bar{t}$ with $m_\chi = 500$ GeV.

To add the $t\bar{t}$ channel in DAMASCO, we modified the publicly available ROOT macro for DAMASCO by adding Eq. (21) to the code along with the parameters in Eqs. (23)-(32). The modified code, and the web application itself, is available for anyone to use at http://cta.gae.ucm.es/gae/damasco.

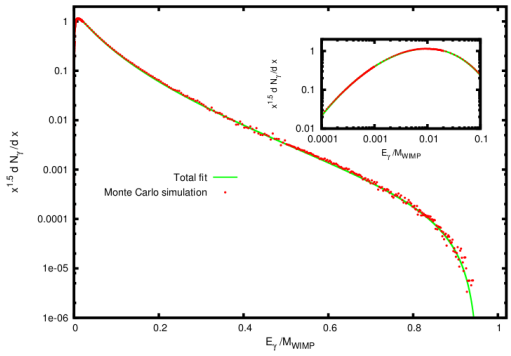

Figure 7: This figure shows the analytical fit to the photon spectra from $\chi\chi \to t\bar{t}$ with $m_\chi = 500$ GeV, compared to the Monte Carlo simulations done in PYTHIA. The figure was extracted from [31].

5 Astrophysical Factors for the Milky Way and Segue 1

The astrophysical factor for annihilating and decaying DM, given by Eq.(2) and (4) respectively, can be interpreted as a measure of how appropriate a source is for indirect DM searches, independent of the particle physics model one choses to describe the DM particle with. The astophysical factor for annihilating dark matter, J_A, crucially depends on the behavior in the region of the dark matter density distribution around $r = 0$, while the astrophysical factor for decaying dark matter, J_D, is less sensitive.

Tables 3-6 show the astrophysical factors we calculated for the Galaxy Center and the dwarf galaxy Segue 1. The parameters for the Einasto density profile for Segue 1 are $D = 23$ kpc (heliocentric distance), $r_E = 0.15$ kpc, $\rho_E = 4.18$ GeV/cm^3 and $\alpha = 0.303$ which were found in [27]. The parameters for the NFW profile and Moore profile were then calculated using Eqs. (8) and (9). For the case of the Milky Way, in [28] one finds $r_{NFW} = r_E = 20$ kpc, $r_I = 5$ kpc, $\rho_{NFW} = 0.345$ GeV/cm^3, $\rho_E = 0.0814$ GeV/cm^3, $\rho_I = 1.56$ GeV/cm^3 and $\alpha = 0.17$ for the Einasto profile (given $r_{NFW,E}$, r_I and α, ρ_{NFW}, ρ_E and ρ_I where determined by the requirement $\rho(r_\odot = 8.5\text{kpc}) = 0.4$ GeV/cm^3 [24]). The parameters for the Moore profile were be calculated by Eqs. (8) and (9). The astrophysical factors were then obtained using $D = r_\odot = 8.5$ kpc.

From Tables 3-4, the uncertainties (in the photon flux) from the lack of knowledge of the DM density distributions is evident. With the Milky Way and $\Delta\Omega = 10^{-3}$, J_A for the Moore profile is roughly a factor of 10^4 larger than for the Isothermal profile, and the difference increases with a smaller $\Delta\Omega$. A small $\Delta\Omega$ is good since it gives a lower background, but in turn magnifies the importance of the details of density profiles. For decaying DM however, the astophysical factors are less dependent on the density profiles, but still, the Moore profile gives significantly larger value than the rest. However, the Moore profile is not as widely used as the NFW or the Einasto profile.

A way to circumvent this problem might be to point the telescope not directly

	Milky Way		
Profile	$\Delta\Omega = 10^{-3}$	$\Delta\Omega = 10^{-4}$	$\Delta\Omega = 10^{-5}$
NFW	58	189	604
Moore	4 960	44 600	396 000
Einasto	91	191	317
Isothermal	0.57	0.57	0.57

Table 3: Values of $\langle J_{\rm A} \rangle_{\Delta\Omega}$ for the center of our Galaxy in units of 10^{23} GeV^2 cm^{-5}.

	Segue 1		
Profile	$\Delta\Omega = 10^{-3}$	$\Delta\Omega = 10^{-4}$	$\Delta\Omega = 10^{-5}$
NFW	0.22	2.0	13.7
Moore	0.46	4.1	38.6
Einasto	0.18	1.6	9.37

Table 4: Values of $\langle J_{\rm A} \rangle_{\Delta\Omega}$ for Segue 1 in units of 10^{23} GeV^2 cm^{-5}.

	Milky Way		
Profile	$\Delta\Omega = 10^{-3}$	$\Delta\Omega = 10^{-4}$	$\Delta\Omega = 10^{-5}$
NFW	20	25	30
Moore	60	109	198
Einasto	27	31	34
Isothermal	5.8	5.8	5.8

Table 5: Values of $\langle J_{\rm D} \rangle_{\Delta\Omega}$ for the center of our galaxy in units of 10^{22} GeV cm^{-2}.

	Segue 1		
Profile	$\Delta\Omega = 10^{-3}$	$\Delta\Omega = 10^{-4}$	$\Delta\Omega = 10^{-5}$
NFW	0.32	1.1	2.4
Moore	0.32	1.1	2.8
Einasto	0.29	1.0	2.3

Table 6: Values of $\langle J_{\rm D} \rangle_{\Delta\Omega}$ for Segue 1 in units of 10^{22} GeV cm^{-2}.

towards the center of the DM distribution. If the telescope instead is pointed towards a region adjacent to the center (without including $r = 0$) where the different density profiles show a similar behavior, the dependence on the choice of density profile is reduced (but so will be the chances to detect any signal at all).

6 Prospects for DM Detection with the MAGIC Telescopes

In this chapter, we investigate the possibilities of DM detection with the MAGIC telescopes. We have chosen the center of the Milky Wasy as our model DM source. Figures 8 - 11 show some examples of the differential flux from various decay channels and WIMP masses in the GeV-TeV range. For the astrophysical factor, we used the Einasto profile, since it is currently the most popular profile in the community, and an angular resolution $\Delta\Omega = 10^{-5}$, corresponding to the resolution of the MAGIC telescopes. The fluxes were computed with Eq.(1) assuming the thermal annihilation cross-section $\langle\sigma v\rangle = 3 \cdot 10^{-26}$ cm^3/s. The same plots also contain the high-energy photon spectrum from the Crab nebula which is used as a "standard candle" for the IACTs. Below the Crab spectrum, there are two lines corresponding to the MAGIC 5σ sensitivity curves for 10 hours and 50 hours of observation [25]. These lines indicate the minimal flux required for a 5σ measurement assuming a Crab-like spectrum (meaning the same shape but different intensity). Since the γ-ray spectra from DM annihilations are not necessarily Crab-like, Figures 8 - 11 are good for order of magnitude estimations, but not for detailed calculations. In most cases in these plots, the DM annihilation photon flux is at least 3 orders of magnitude lower than the 50 hour sensitivity curve. Eq.(20) shows that the required observation time is inversely proportional to the square of the flux, meaning that these fluxes at first glance should require at least $50 \cdot 10^6$ hours ($\sim$ 5700 years!) of observation.

In order to obtain more accurate estimations of the time MAGIC needs to detect a DM signal of a 5σ level, we performed more detailed calculations. The observation times where calculated using Eq.(20) for $S = 5$. For $R_{\rm off}$ and $R_{\rm exc}$ we can write

$$R_{\rm off}(E_{\rm Min}, E_{\rm Max}) = \int_{E_{\rm Min}}^{E_{\rm Max}} {\rm d}E \frac{{\rm d}R_{\rm off}}{{\rm d}E}, \tag{33}$$

$$R_{\rm exc}(E_{\rm Min}, E_{\rm Max}) = \int_{E_{\rm Min}}^{E_{\rm Max}} {\rm d}E A_{\rm eff}(E) \frac{{\rm d}\Phi^\gamma}{{\rm d}E} \tag{34}$$

where $E_{\rm Min}$ and $E_{\rm Max}$ denote the lower and upper limit on the energy interval under consideration. $A_{\rm eff}$ is the effective area which in general depends on the photon energy and ${\rm d}\Phi^\gamma/{\rm d}E$ is the expected γ-ray flux and is given by Eqs.(1) and (3) in the case of indirect DM searches. This gives

$$t_{\rm obs} = 50 \frac{\int_{E_{\rm Min}}^{E_{\rm Max}} {\rm d}E \frac{{\rm d}R_{\rm off}}{{\rm d}E}}{\left[\int_{E_{\rm Min}}^{E_{\rm Max}} {\rm d}E A_{\rm eff}(E) \frac{{\rm d}\Phi^\gamma}{{\rm d}E}\right]^2}. \tag{35}$$

The effective area $A_{\rm eff}$ and the off-event rate ${\rm d}R_{\rm off}/{\rm d}E$ are those of the MAGIC telescopes which were taken from [25]. The upper limit for the energy interval is chosen as $E_{\rm Max} = m_\chi$ since this is where the characteristic cut-off occurs. The lower limit is $E_{\rm Min} = 100$ GeV which is the standard analysis threshold for MAGIC.

Our results are shown in Table 7. This table contains the required observation times for measuring a photon excess from DM annihilations depending on the WIMP mass and annihilation channel. Table 7 shows that for a light

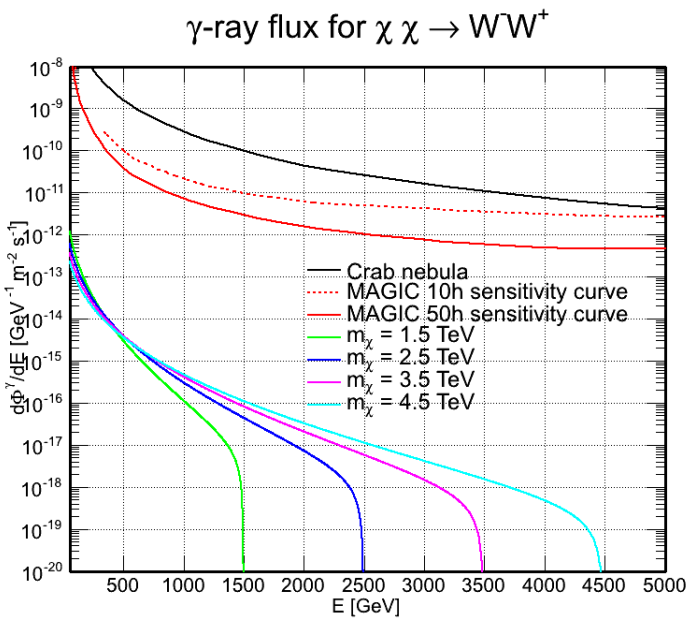

Figure 8: The colored lines show the photon differential flux for $\chi\chi \to W^-W^+$ from the GC when applying the Einasto profile and $\Delta\Omega = 10^{-5}$ (corresponding to the MAGIC angular resolution). The black line shows the Crab Nebula flux. The red lines show the MAGIC 5σ sensitivity lines for 10 hours and 50 hours of observation time respectively. A thermal annihilation cross-section is assumed.

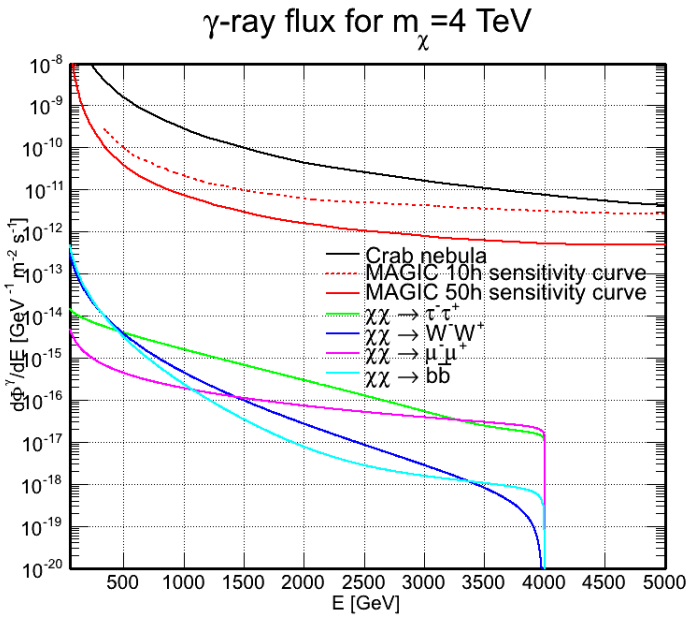

Figure 9: The colored lines show the photon differential flux for four different annihilation channels with a fixed WIMP mass of 4 TeV. The rest as in Fig. 8. These spectra could also be interpreted as decaying DM with a decay time of order 10^{27} s which is realized by equating Eq.(1) and Eq.(3).

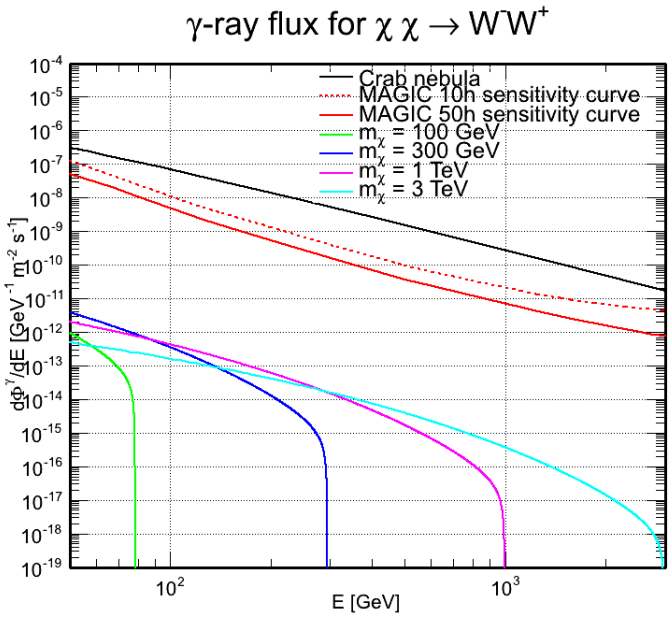

Figure 10: The colored lines show the photon differential flux for $\chi\chi \to W^-W^+$ for different m_χ. The rest as in Fig. 8.

WIMP (m_χ = a few 100 GeV), the annihilation channel $\chi\chi \to \tau^+\tau^-$ is easiest to detect, while $\chi\chi \to W^+W^-$ is most promising for WIMPs with a mass higher than 5 TeV.

However, despite the discouraging results in Figures 8 - 11 and Table 7, the hope of detecting photons from DM annihilations is not at all lost. There exist several effects one can take into account which dramatically boost the photon flux.

- One effect is the *Sommerfeld enhancement* which concerns the DM annihilation cross-section. According to some authors [33], for a WIMP mass in the range of 100 GeV – 1 TeV, the annihilation cross-section (and thus the photon flux) may be boosted by a factor of 7–90.

- It has been argued ([34],[35]) that central DM density in the GC can be dramatically increased when baryonic gas is taken into account. For example for the NFW profile, the flux from DM annihilations, coming from the GC, is boosted by a factor $\sim 10^3$ [35].

- It has been claimed that an additional boost factor can come from substructures in the DM halos [36], [37]. In this work, we have assumed smooth density profiles, but the actual halos may contain dense "clumps" of DM which can be shown to increase the astrophysical factors for annihilating DM. Though, these boost factors are usually $\mathcal{O}(1)$.

Taking into account the small duty cycle of IACTs (normally $\sim$ 1000 hours of observation is available per year), and the high number if interesting targets,

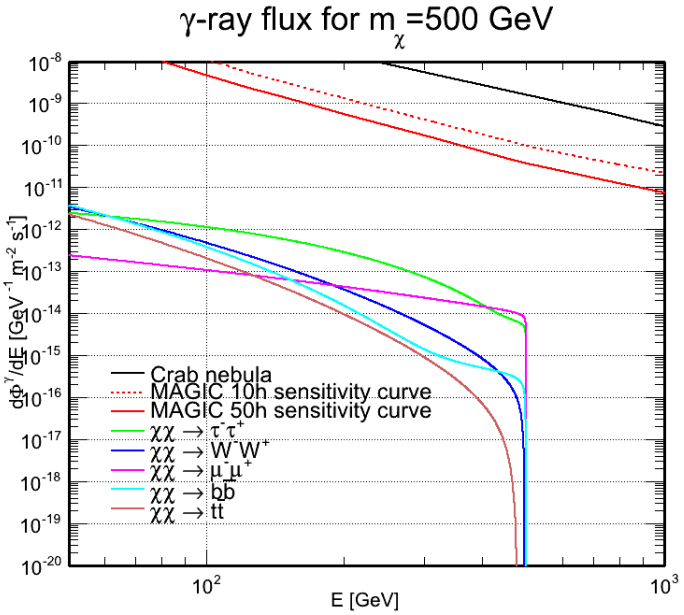

Figure 11: The colored lines show the photon differential flux for four different annihilation channels with a fixed WIMP mass of 500 GeV. The rest as in Fig. 8. These spectra could also be interpreted as decaying DM with a decay time of order 10^{26} s which is realized by equating Eq.(1) and Eq.(3).

m_χ (GeV):	260	500	1000	5000	10000	15000
$\mu^+\mu^-$	$4.8 \cdot 10^7$	$8.3 \cdot 10^7$	$3.2 \cdot 10^8$	$1.3 \cdot 10^{10}$	$9.8 \cdot 10^{10}$	$3.4 \cdot 10^{11}$
$\tau^+\tau^-$	$4.5 \cdot 10^6$	$3.3 \cdot 10^6$	$7.7 \cdot 10^6$	$3.5 \cdot 10^8$	$2.7 \cdot 10^9$	$1.0 \cdot 10^{10}$
W^+W^-	$5.6 \cdot 10^8$	$9.2 \cdot 10^7$	$4.9 \cdot 10^7$	$1.9 \cdot 10^8$	$6.9 \cdot 10^8$	$1.7 \cdot 10^9$
$b\bar{b}$	$3.3 \cdot 10^9$	$5.0 \cdot 10^9$	$8.3 \cdot 10^7$	$1.6 \cdot 10^8$	-	-

Table 7: The observation times in hours required for a 5σ measurement of a photon flux excess in the energy range between 100 GeV and m_χ for different annihilation channels and WIMP masses. The source is assumed to be the Milky Way with an Einasto profile without any boost factor. A thermal annihilation cross-section is assumed. The telescope dependent parameters ($\Delta\Omega$, $A_{\rm Eff}(E)$ and $\mathrm{d}R_{\rm off}/\mathrm{d}E$) are those of MAGIC. See text for details.

rarely more than 100 hours are consented for observations of one object. The boost factor needed in order to achieve a 5σ detection in 100 hours are e.g. ~ 180 for $\chi\chi \to \tau^+\tau^-$ and $m_\chi = 500$ GeV, and ~ 2600 for $\chi\chi \to W^+W^-$ with $m_\chi = 10$ TeV. Such a high boost factor is difficult to accomplish, and this shows the difficulty of proving the existence of DM with this technique.

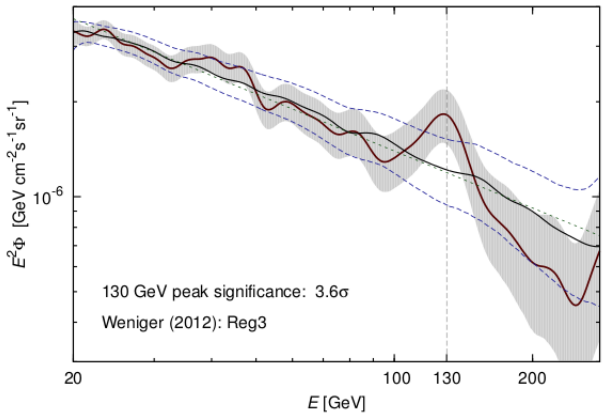

Figure 12: Estimated γ-ray flux for the region in Figure 13 with the 95% confidence level (CL) error band. The black solid line shows the estimated background, which fluctuates around a simple power-law spectrum with power 2.6 (dotted line). The blue dashed lines are the 95% CL limits for statistical fluctuations of the background. This figure was extracted from [39].

7 130 GeV γ-ray Line From Decaying Dark Matter

Recently, an analysis of public data of gamma-rays from the Milky Way measured by the Fermi Large Area Telescope (LAT) showed an indication of a gamma-ray line at $E_\gamma \approx 130$ GeV with a statistical significance of 3.3σ [38]. A similar signal was later confirmed in [39] (see Figure 12.). In [38], the flux was interpreted as a result of $\chi\chi \to \gamma\gamma$ with a dark matter particle mass of $129.8 \pm 2.4^{+7}_{-13}$ GeV and a partial annihilation cross-section of $\langle\sigma v\rangle = (1.27 \pm 0.32^{+0.18}_{-0.28}) \cdot 10^{-27}$ cm^{3}s^{-1} (i.e. a tenth of the expected total annihilation cross-section) when using the Einasto density profile, Eq.(7), for the Milky Way dark matter halo.

Other interpretations, such as $\chi\chi \to \gamma X$, have also been studied [39], as well as the possibility that the line comes from decaying DM [40]. It has also been discussed that the line may be a feature of the diffuse background with either astrophysical or instrumental origin [41]. Attempts have been made to see this line in dShps, but no such line was observed [42].

In this section, we further investigate the possibility that the 130 GeV line originates from decaying dark matter. The first section takes on a model-independent approach, in which the DM decay times required to produce the line are calculated, depending on the decay mode and density profile for the Milky Way. The second section deals with a particular model, namely decaying gravitinos.

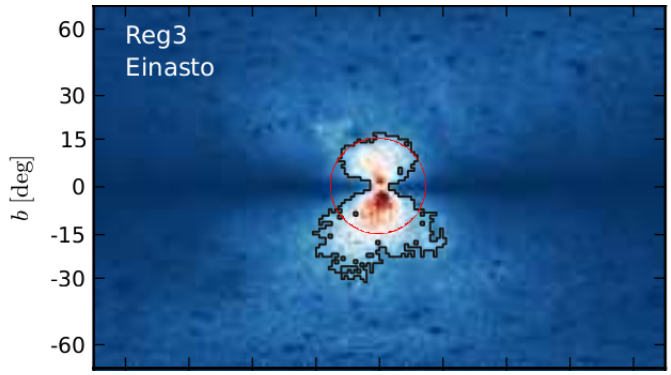

Figure 13: The region enclosed within the *black* line is the region used in the original article [38] (and which was chosen since it maximizes the signal to noise ratio). The region within the *red* circle is the region used in this work.

7.1 A Model-independent Approach

Figure 13 shows one of the four regions which were analyzed in [38], and for which the Einasto density profile was applied. The region was chosen in order to maximize the signal to background ratio, hence its complicated shape. In this work, the same region will be approximated by a circular region centered on the GC with $\theta_{Max} = 15^\circ$ (meaning that $\Delta\Omega = 0.214$). Applying the Einasto profile, the astrophysical factor for annihilating dark matter in this region is calculated with Eq.(2).

$$\langle J_{\rm A}\rangle_{\Delta\Omega} = 4.972 \cdot 10^{23}{\rm GeV}^2{\rm cm}^{-5} \tag{36}$$

The astrophysical factors for the same region, but for decaying dark matter were calculated using Eq.(4). Applying various density profiles, the astrophysical factors are

$$\begin{aligned}
\langle J_{D,Einasto}\rangle_{\Delta\Omega} &= 1.085 \cdot 10^{23}{\rm GeVcm}^{-2}, &(37)\\
\langle J_{D,NFW}\rangle_{\Delta\Omega} &= 9.206 \cdot 10^{22}{\rm GeVcm}^{-2}, &(38)\\
\langle J_{D,Moore}\rangle_{\Delta\Omega} &= 1.236 \cdot 10^{23}{\rm GeVcm}^{-2}, &(39)\\
\langle J_{D,Isothermal}\rangle_{\Delta\Omega} &= 5.476 \cdot 10^{22}{\rm GeVcm}^{-2}. &(40)
\end{aligned}$$

Let $M_1 = 129.8 \pm 2.4^{+7}_{-13}$ GeV denote the dark matter particle mass for $\chi\chi \to \gamma\gamma$, and M_2 the corresponding dark matter particle mass for $\chi \to \gamma X$. In order for the line to appear at the same energy, the relation between M_1 and M_2 is fixed by $E_1^\gamma = E_2^\gamma \equiv E^\gamma$ in Eq.(12) and Eq.(13)

$$M_2 = M_1\left(1 + \sqrt{1 + \frac{m_X^2}{M_1^2}}\right). \tag{41}$$

The dark matter decay width can be determined by requiring that ${\rm d}\Phi_{\rm A}^\gamma/{\rm d}E = {\rm d}\Phi_{\rm D}^\gamma/{\rm d}E$. Equating Eq.(1) and Eq.(3) for $\chi\chi \to \gamma\gamma$ and $\chi \to \gamma X$ yields

$$\frac{1}{8\pi M_1^2}\langle\sigma v\rangle\delta(E - E^\gamma)\Delta\Omega\langle J_{\rm A}\rangle_{\Delta\Omega} =$$

Profile	$\chi \to \gamma\gamma$	$\chi \to \gamma\nu$	$\chi \to \gamma Z$	$\chi \to \gamma h$
Einasto	$2.23^{+2.30}_{-0.82}$	$1.11^{+1.15}_{-0.41}$	$1.00^{+1.06}_{-0.38}$	$0.933^{+1.000}_{-0.365}$
NFW	$1.83^{+1.89}_{-0.67}$	$0.916^{+0.946}_{-0.337}$	$0.824^{+0.872}_{-0.316}$	$0.767^{+0.822}_{-0.300}$
Moore	$2.54^{+2.63}_{-0.93}$	$1.27^{+1.31}_{-0.48}$	$1.14^{+1.21}_{-0.44}$	$1.06^{+1.14}_{-0.42}$
Isothermal	$1.13^{+1.16}_{-0.41}$	$0.563^{+0.581}_{-0.207}$	$0.507^{+0.536}_{-0.194}$	$0.507^{+0.505}_{-0.184}$
M_2 (GeV)	$259.6^{18.8}_{-30.8}$	$259.6^{18.8}_{-30.8}$	$288.4^{+17.2}_{-27.7}$	$310.0^{+16.3}_{-26.2}$

Table 8: Decay lifetimes in units of 10^{28} s obtained when interpreting the results presented in [38] as originating from decaying dark matter for different density profiles for the Milky Way. The Higgs mass is assumed to be 125 GeV.

$$\frac{1}{4\pi M_2}\Gamma_{\chi\to\gamma X} a\delta(E-E^\gamma)\Delta\Omega\langle J_{\rm D}\rangle_{\Delta\Omega},$$

or

$$\Gamma_{\chi\to\gamma X} = \frac{1+\sqrt{1+m_X^2/M_1^2}}{2}\cdot\frac{\langle\sigma v\rangle}{aM_1}\cdot\frac{\langle J_{\rm A}\rangle_{\Delta\Omega}}{\langle J_{\rm D}\rangle_{\Delta\Omega}}. \tag{42}$$

As before, $a = 2$ when X is a photon, and $a = 1$ otherwise. Since the lifetime τ is the inverse of the decay width Γ, the lifetime depending on the density profile can be calculated through Eq.(42) using the different values of $\langle J_{\rm D}\rangle_{\Delta\Omega}$ for the corresponding profiles, Eq.(37)-(40). One thereby obtains the lifetimes shown in Table 8. Here, the assumed Higgs mass is 125 GeV, which is the value in between the ATLAS prediction [43], 126 GeV, and the CMS prediction [44], 124 GeV. From this table, one concludes that if the 130 GeV line is to be explained by a dark matter decay of the type $\chi \to \gamma X$, the lifetime should be in the range of $3 \cdot 10^{27}$ s (lower limit for $\chi \to \gamma H$ with the isothermal profile) to $5 \cdot 10^{28}$ s (upper limit for $\chi \to \gamma\gamma$ with the Moore profile), i.e. much longer than the age of the universe which is $\sim 10^{17}$ s. With such a long lifetime, the dark matter decay would not have a significant impact on standard cosmology. The lifetime is well above the lower limit one can obtain from the CMB [45]. These lifetimes are also not ruled out by the more stringent constraints that has been derived from several gamma ray measurements [46].

7.2 A 130 GeV Line from Gravitino Decays

In [47], a model for R-parity violating gravitino decay is discussed as an explanation of the positron excess measured by PAMELA [48]. This model contains several gravitino decay channels, but only one where the photon is among the decay products. In this section, the same model is applied to the 130 GeV line. The gravitino would decay to a photon and a neutrino, thus produce a line at $\sim$130 GeV in the photon spectra if the gravitino mass is $\sim$260 GeV.

In [47], the R-parity violating couplings of the gravitino ψ to SM particles are described by

$$\mathcal{L}_{\rm eff} = \frac{i\kappa}{\sqrt{2}M_{\rm Pl}}\left\{\bar{l}\gamma^\lambda\gamma^\nu D_\nu\phi\psi_\lambda + \frac{i}{2}\bar{l}\gamma^\lambda(\xi_1 g' Y B_{\mu\nu} + \xi_2 g W_{\mu\nu})\sigma^{\mu\nu}\phi\psi_\lambda\right\} + \text{h.c.}, \tag{43}$$

where the parameters κ, ξ_1 and ξ_2 have suppressed flavor indices (this of course also the case for the lepton doublets l). The Higgs and the lepton doublets read

$$\phi = \begin{pmatrix} v + \frac{h}{\sqrt{2}} \\ 0 \end{pmatrix}, \tag{44}$$

$$l_i = \begin{pmatrix} \nu_i \\ e_i \end{pmatrix}, \tag{45}$$

where i indicates flavour. The covariant derivative D_μ contains the U(1) and SU(2) SM gauge fields,

$$D_\mu = \partial + ig'YB_\mu + \frac{1}{2}ig\sigma^I W_\mu^I \tag{46}$$

where σ^I are the Pauli matrices and Y is the weak hypercharge which equals $-1/2$ for the gravitino. The corresponding field strengths are

$$B_{\mu\nu} = \partial_\mu B_\nu - \partial_\nu B_\mu, \tag{47}$$

$$W_{\mu\nu} = \partial_\mu W_\nu - \partial_\nu W_\mu + i[W_\mu, W_\nu]. \tag{48}$$

The different possibilities for R-parity violating couplings for the gravitino are constrained by

$$(i\gamma^\mu\partial_\mu - m_{3/2})\psi_\nu = 0, \tag{49}$$

which is the Dirac equation, and

$$\gamma^\mu\psi_\mu = 0, \tag{50}$$

$$\partial^\mu\psi_\mu = 0. \tag{51}$$

A derivation of these constraints can for example be found in the PhD thesis of T. Moroi [49], chapter 4, and it is via these constraints that the form of Eq.(43) is obtained in [47].

On writing out all the terms in Eq.(43), one obtains terms for the decays $\psi_{3/2} \to h\nu_i, Z\nu_i, W^\pm e_i^\mp$ and $\psi_{3/2} \to \gamma\nu_i$, where the last one would produce a line in the photon spectra. The corresponding term in the Lagrangian for this decay is

$$-\frac{\kappa}{\sqrt{2}M_{\rm Pl}} m_Z \xi_\gamma (\partial_\mu A_\nu)\bar{\nu}\gamma^\lambda\sigma^{\mu\nu}\psi_\lambda, \tag{52}$$

with

$$\xi_\gamma = \sin\theta_{\rm W}\cos\theta_{\rm W}(\xi_2 - \xi_1) \tag{53}$$

where $\theta_{\rm W}$ is the Weinberg angle. The Lagrangian Eq.(43) also contains the Hermitian conjugate of the term (52) which corresponds to $\psi_{3/2} \to \gamma\bar{\nu}_i$. From Eq.(52) it follows (see [47]) that the decay width for $\psi_{3/2} \to \gamma\nu_i$ is

$$\Gamma(\psi_{3/2} \to \gamma\nu_i) = \kappa_i|\xi_{\gamma i}|^2 \frac{m_Z^2 m_{3/2}^3}{64\pi M_{\rm Pl}^2}. \tag{54}$$

Since half of the photons in the 130 GeV line should come from $\psi_{3/2} \to \gamma\bar{\nu}_i$, the total decay width contributing to the γ-ray line is

$$\Gamma(\psi_{3/2} \to \gamma\nu_{1-3}, \gamma\bar{\nu}_{1-3}) = \sum_{i=1}^{3} 2\kappa_i|\xi_{\gamma i}|^2 \frac{m_Z^2 m_{3/2}^3}{64\pi M_{\rm Pl}^2}. \tag{55}$$

For example, if one uses the Einasto profile for the Milky Way DM halo, one can according to table 8 interpret the 130 GeV γ-ray line as originating from $\psi_{3/2} \to \gamma\nu_i$ with $\Gamma^{-1} = 1.11^{+1.15}_{-0.41} \cdot 10^{28}$ s and $m_{3/2} = 259.6^{18.8}_{-30.8}$ GeV. This fixes

$$\sum_{i=1}^{3} \kappa_i |\xi_{\gamma i}|^2 = 6.1^{+8.0}_{-3.7} \cdot 10^{-24} \mathrm{GeV}^{-2}. \tag{56}$$

Another decay channel present in Eq. (43) is $\psi_{3/2} \to W^{\pm} e_i^{\mp}$. Both the lepton and the W boson will produce a continuous photon spectrum similar to those that are computed in DAMASCO. Let E_W and E_l denote the energies of the W and the lepton in rest frame after the decay of $\psi_{3/2}$. Neglecting the lepton masses, it is straight forward to show that

$$E_W = \frac{m_{3/2}^2 + m_W^2}{2m_{3/2}}, \tag{57}$$

$$E_l = \frac{m_{3/2}^2 - m_W^2}{2m_{3/2}}. \tag{58}$$

The photon spectrum from $\psi_{3/2} \to W^{\pm} e_i^{\mp}$ will thus be the sum of two spectra with cut-offs at $E_W \sim 142$ GeV and $E_l \sim 117$ GeV respectively, assuming $m_{3/2} = 259.6$ GeV. Following the same line of thought, the decay $\psi_{3/2} \to Z\nu_i$ will produce a spectra with a cut-off at ~ 146 GeV.

7.3 Conclusions

In this section we have analyzed the recently claimed 130 GeV γ-ray line in the case it comes from a decaying dark matter particle. The region of the GC used in [38] is relatively large, the computed astrophysical factors for decaying dark matter for this region are all roughly within a factor of two. Interpreting the flux from this region as coming from decaying dark matter gives decay times of order 10^{28} s, depending on the decay channel and density profile. The decay times and the corresponding DM particle mass for the different density profiles are shown in Table 8.

If the 130 GeV line comes from a decaying WIMP, it may be a good idea to look for a cut-off in the γ-ray spectra at $E^{\gamma} \approx 260$ GeV. The gravitinos would be thermally produced, and should therefore have a thermal annihilation cross-section. The first column in table 7 shows the observation times (without a boost factor) required to observe the γ-ray flux below 260 GeV that would be produced depending on the annihilation channel. For this to be detectable by the MAGIC telescopes during 100 hours, one needs to assume a boost factor between ~ 200 ($\chi\chi \to \tau^+\tau^-$) and ~ 5700 ($\chi\chi \to b\bar{b}$). This is realized by considering that the observation time is inversely proportional to the square of the γ-ray flux, see Eq.(20).

We have also discussed a model for decaying gravitinos. On interpreting the 130 GeV line as coming from $\psi_{3/2} \to \gamma\nu_i, \gamma\bar{\nu}_i$ we calculated a value for the coupling of the (anti-)neutrino-photon-gravitino vertex.

A γ-ray line can have many different interpretations, and additional pieces of information are needed in order to establish that the line for example originates from gravitino decays. Since every photon from a gravitino decay must be

accompanied by a neutrino, the hypothesis that the 130 GeV line originates from gravitino decays can be falsified by the non-observation of a line in the neutrino spectrum at 130 GeV with a similar intensity.

8 Summary

This work has treated the method of indirect DM detection using IACTs, which in the upcoming years may provide important information about the nature of DM. In Chapter 2, we gave a non-technical general overview of the DM problem today, while in Chapter 3 we described in more detail the different issues that are connected to detection of γ-rays from DM annihilations/decays using IACTs.

In Chapter 4, we calculated astrophysical factors (for decaying and annihilating DM) for the Milky Way and the dwarf galaxy Segue 1. The astrophysical factors were calculated using the typical angular resolution of IACTs and satellite based γ-ray detectors ($\Delta\Omega = 10^{-3}$, 10^{-4} and 10^{-5}). Our results are shown in Tables 3-6. We showed that when $\Delta\Omega$ decreases, the difference in the astrophysical factors for different DM density profiles increases dramatically in the case of annihilating DM. Today, this constitutes the major uncertainty in indirect DM searches with IACTs and thus calls for more accurate descriptions of DM halos.

The prospects for DM detection with the MAGIC telescopes were then discussed in Chapter 5. Here, we calculated γ-ray fluxes from the GC using the formulae from Chapter 2. We computed the photon spectra with the DAMASCO code and used astrophysical factors for the GC that were calculated in Chapter 3. The flux for different annihilation channels were compared to the γ-ray flux from the Crab nebula and the 50 hours and 10 hours MAGIC sensitivity curves. We thereby calculated the required observation time for 5σ detections, assuming different annihilation channels and WIMP masses, and without assuming a boost factor. Throughout chapter, we assumed the thermal annihilation cross-section $\langle\sigma v\rangle = 3 \cdot 10^{-26}\text{cm}^3/\text{s}$, and the Einasto profile for the Milky Way. The results are shown in table 7. For the different cases we treated, the best case scenario ($\chi\chi \to \tau^+\tau^-$ with $m_\chi = 500$ GeV) required a boost factor of ~ 180 for a 5σ detection with an observation time of 100 hours.

In Chapter 6 we analyzed the recently observed 130 GeV line in the case it originates from decaying DM. We calculated the life times for the decay channels $\chi \to \gamma\gamma$, $\gamma\nu$, γZ and γh, and the corresponding WIMP masses depending on the density profile applied to the Milky Way. The results are in Table 8. Thereafter, we discussed a model for R-parity violating gravitino decays. By interpreting the 130 GeV line as coming from $\psi_{3/2} \to \gamma\nu$ we obtained the coupling for the corresponding vertex. Another signature this model predict is a similar line in the neutrino spectrum which could be measured by the IceCube neutrino telescope. If the line comes from a decaying WIMP, one should look for a cut-off in the photon spectra at $E^\gamma \approx 260$ GeV. From the results in Chapter 5, we conclude that for this cut-off to be measurable with the MAGIC telescopes, a boost factor in the range of 200 - 5700 (depending on the annihilation channel) is needed.

References

[1] Garrett, K., Dūda, G. *Dark Matter: A Primer* arXiv:1006.2483v1 [hep-ph]

[2] Bergström, L *Dark Matter Evidence, Particle Physics Candidates and Detection Methods* arXiv:1205.4882v1 [astro-ph.HE]

[3] WMAP Collaboration *Seven-Year Wilkinson Microwave Anisotropy Probe (WMAP) Observations: Cosmological Interpretation* arXiv:1001.4538v3 [astro-ph.CO]

[4] Steigman, G., Dasgupta, B., Beacom, J. F. *Precise Relic WIMP Abundance and its Impact on Searches for Dark Matter Annihilation* arXiv:1204.3622v2 [hep-ph]

[5] FERMI collaboration *Constraining Dark Matter Models from a Combined Analysis of Milky Way Satellites with the Fermi Large Area Telescope* arXiv:1108.3546v3 [astro-ph.HE]

[6] K. Nakamura *et al.* (Particle Data Group), J. Phys. G 37, 075021 (2010)

[7] Perez, P. F., Spinner, S. *The Minimal Theory for R-parity Violation at the LHC* arXiv:1201.5923v2 [hep-ph]

[8] Super-Kamiokande Collaboration *Search for Proton Decay via* $p \to e^+\pi^0$ *and* $p \to \mu^+\pi^0$ *in a Large Water Cherenkov Detector* arXiv:0903.0676v2 [hep-ex]

[9] Ishiwata, K., Matsumoto, S., Moroi, T. *High Energy Cosmic Rays from the Decay of Gravitino Dark Matter* arXiv:0805.1133v2 [hep-ph]

[10] Akimov *et al. WIMP-nucleon cross-section results from the second science run of ZEPLIN-III* arXiv:1110.4769v2 [astro-ph.CO]

[11] Nieto, D. *Dark Matter Constraints from High Energy Astrophysical Observations* (PhD thesis)

[12] Amelino-Camelia, G., Ellis, J., Mavromatos, N. E., Nanopoulos, D. V. *Distance Measurement and Wave Dispersion in a Liouville-String Approach to Quantum Gravity* arXiv:hep-th/9605211v1

[13] Oh, S. H. *et al. Dark and Luminous Matter in THINGS Dwarf Galaxies* arXiv:1011.0899v2 [astro-ph.CO]

[14] MAGIC Collaboration *MAGIC Gamma-ray Telescope Observation of the Perseus Cluster of Galaxies: implications for cosmic rays, dark matter, and NGC1275* arXiv:0909.3267v3 [astro-ph.HE]

[15] H.E.S.S. Collaboration *Search for a Dark Matter annihilation signal from the Galactic center halo with H.E.S.S* arXiv:1103.3266v1 [astro-ph.HE]

[16] Aleksic, J., Doro, M., Lombardi, S., Nieto, D., Fornasa, M. *Segue 1: the best dark matter candidate dwarf galaxy surveyed by MAGIC* arXiv:1109.6781v2 [astro-ph.CO]

[17] Springel *et al. The Aquarius Project: the subhalos of galactic halos* arXiv:0809.0898v1 [astro-ph]

[18] Nieto *et al. The search for galactic dark matter clump candidates with Fermi and MAGIC* arXiv:1109.5935v1 [astro-ph.HE]

[19] Navarro, J. F., Frenk, C. S. & White S. D. M. *A Universal Density Profile from Hierarchial Clustering* arXiv:9611107v4 [astro-ph]

[20] Navarro *et al. The Diversity and Similarity of Simulated Cold Dark Matter Halos* arXiv:0810.1522v2 [astro-ph]

[21] Sofue, Y., Honma, M., Omodaka, T. *Unified Rotation Curve of the Galaxy – Decomposition into de Vaucouleurs Bulge, Disk, Dark Halo, and the 9-kpc Rotation Dip* – arXiv:0811.0859v2 [astro-ph]

[22] Cen, R. *Decaying Cold Dark Matter Model and Small-Scale Power* arXiv:astro-ph/0005206v2

[23] de Blok, W. J. G. 2009 *The Core-Cusp Problem* arXiv:0910.3538v1

[24] Catena R., Ullio, P. *A novel determination of the local dark matter density* arXiv:0907.0018v2 [astro-ph.CO]

[25] MAGIC Collaboration *Performance of the MAGIC stereo system obtained with Crab Nebula data* arXiv:1108.1477v2

[26] Prada, F., Klypin, A., Flix Molina, J., Martinéz, M., Simonneau, E., *Astrophysical inputs on the SUSY dark matter annihilation detectability* arXiv:astro-ph/0401512v1

[27] MAGIC Collaboration *Searches for Dark Matter annihilation signatures in the Segue 1 satellite galaxy with the MAGIC-I telescope* arXiv:1103.0477 [astro-ph.HE]

[28] FERMI Collaboration *Fermi LAT Search for Dark Matter in Gamma-ray Lines and the Inclusive Photon Spectrum* arXiv:1205.2739v1 [astro-ph.HE]

[29] Li, T., Ma, Y., *Analysis Methods for Results in Gamma-Ray Astronomy* The Astrophysical Journal 272 (1983) 317-324

[30] Antcheva, I., Ballintijn, M., Bellenot, B., Biskup, M., Brun, R., Buncic, N., Canal, P., Casadei, D. *et al. ROOT: A C++ framework for petabyte data storage, statistical analysis and visualization* Comput. Phys. Commun. **180** (2009) 2499.

[31] Cembranos *et al. Photon spectra from WIMP annihilation* arXiv:1009.4936v2 [hep-ph]

[32] Rajaraman, A., Tait, T.M.P., Whiteson, D. *Two Lines or Not Two Lines? That is the Question of Gamma Ray Spectra* arXiv:1205.4723v1 [hep-ph]

[33] Feng, J. L., Kaplinghat, M., Yu, H. *Sommerfeld Enhancements for Thermal Relic Dark Matter* arXiv:1005.4678v3 [hep-ph]

[34] Gnedin, O. Y., Kravtsov, A. V., Klypin, A. A., Nagai, D. *Response of dark matter halos to condensation of baryons: cosmological simulations and improved adiabatic contraction model* arXiv:astro-ph/0406247v2

[35] Prada, F. , Klypin, A., Flix, J., Martinez M., Simonneau, E. *Astrophysical inputs on the SUSY dark matter annihilation detectability* arXiv:astro-ph/0401512v1

[36] Stoehr, F., White, S. D. M., Springel, V., Tormen, G., Yoshida, N., Mon. Not. **R** Astron. Soc. *345*, 1313 (2003)

[37] Klypin, A., Kravtsov, A. V., Valezuela, O., Prada, F., Astophys. J. **552**, 82 (1999)

[38] Weniger, C. *A Tentative Gamma-Ray Line from Dark Matter Annihilation at the Fermi Large Area Telescope* arXiv:1204.2797v1 [hep-ph]

[39] Tempel, E., Hektor, A., Raidal, M. *Fermi 130 GeV gamma-ray excess and dark matter annihilation in sub-halos and in the Galactic centre* arXiv:1205.1045 [hep-ph]

[40] Kyae, B., Park, J. *130 GeV Gamma-Ray Line from Dark Matter Decay* arXiv:1205.4151v1 [hep-ph]

[41] Boyarsky, A., Malyshev, D., Ruchayskiy, O. *Spectral and spatial variations of the diffuse gamma-ray background in the vicinity of the Galactic plane and possible nature of the feature at 130 GeV* arXiv:1205.4700v1 [astro-ph.HE]

[42] Geringer-Sameth, A., M. Koushiappas, S. M. *Dark matter line search using a joint analysis of dwarf galaxies with Fermi* arXiv:1206.0796v1 [astro-ph.HE]

[43] ATLAS Collaboration *Combined search for the Standard Model Higgs boson using up to 4.9 fb-1 of pp collision data at sqrt(s) = 7 TeV with the ATLAS detector at the LHC* arXiv:1202.1408v3 [hep-ex]

[44] CMS Collaboration *Combined results of searches for the standard model Higgs boson in pp collisions at sqrt(s) = 7 TeV* arXiv:1202.1488v1 [hep-ex]

[45] Ichiki, K., Oguri, M., Takahashi, K. *WMAP Constraints on Decaying Cold Dark Matter* arXiv:astro-ph/0403164v2

[46] Cirelli, M. *et al. Gamma ray constraints on Decaying Dark Matter* arXiv:1205.5283v1 [astro-ph.CO]

[47] Buchmüller, W., Ibarra, A., Shindou, T., Takayama, F., Tran, D. *Probing Gravitino Dark Matter with PAMELA and Fermi* arXiv:0906.1187v3 [hep-ph]

[48] PAMELA collaboration *Observation of an anomalous positron abundance in the cosmic radiation* arXiv:0810.4995v1 [astro-ph]

[49] Moroi, T., *Effects of the Gravitino on the Inflationary Universe* arXiv:hep-ph/9503210v1